Immuno-genomic-radiomics to predict response of biliary tract cancer to camrelizumab plus GEMOX in a single-arm phase II trial

Authors

Qiu-Ping Liu, **Jie Tang**, Yi-Zhang Chen, Fen Guo, Ling Ma, Lan-Lan Pan, Yi-Tong Tian, Xiao-Feng Wu, Yu-Dong Zhang, Xiao-Feng Chen

Correspondence

njmu_lqp@163.com (Q.-P. Liu), lytangj@126.com (J. Tang), yizhangchen@njmu.edu.cn (Y.-Z. Chen), guof123@126.com (F. Guo), maling@njmu.edu.cn (L. Ma), zjpanlanlan@163.com (L.-L. Pan), 835385247@qq.com (Y.-T. -Tian), wuxf@njmu.edu.cn (X.-F. Wu), zhangyd3895@njmu.edu.cn (Y.-D. Zhang), chenxiaofengnjmu@163.com (X.-F. Chen).

Graphical abstract

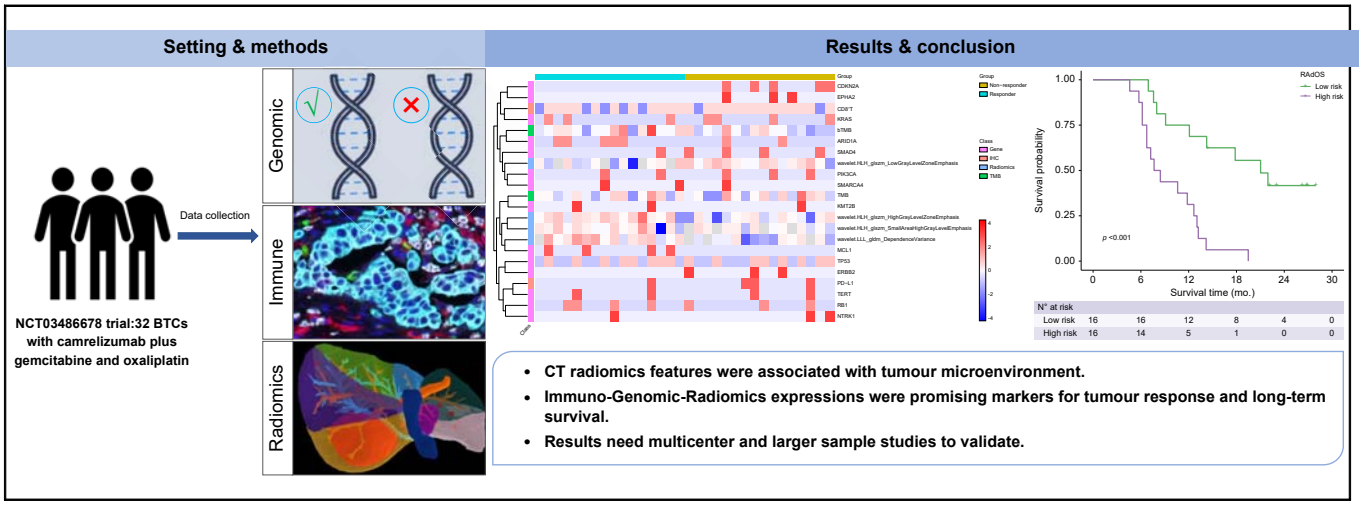

Highlights

- IGR features were collected in patients with advanced BTC receiving camrelizumab plus GEMOX therapy.
- Radiomics were correlated with immuno-genomic biomarkers.
- IGR features were predictors of treatment response and survival outcome.

Impact and implications

Immunotherapy is an alternative for the treatment of advanced BTC, whereas tumour response is heterogeneous. In a *post hoc* analysis of the single-arm phase II clinical trial (NCT03486678), we found that CT radiomics features were associated with the tumour microenvironment and that IGR expression was a promising marker for tumour response and long-term survival.

https://doi.org/10.1016/j.jhepr.2023.100763

Research article

JHEP|Reports

Immuno-genomic-radiomics to predict response of biliary tract cancer to camrelizumab plus GEMOX in a single-arm phase II trial

Qiu-Ping Liu,[1,†] **Jie Tang**,[2,†] Yi-Zhang Chen,[3] Fen Guo,[4,5] Ling Ma,[3] Lan-Lan Pan,[3] Yi-Tong Tian,[3] Xiao-Feng Wu,[6,*] Yu-Dong Zhang,[1,*] Xiao-Feng Chen[3,5,7,*]

[1]Department of Radiology, The First Affiliated Hospital of Nanjing Medical University, Nanjing, Jiangsu, China; [2]Department of Oncology, Liyang People's Hospital, Liyang, China; [3]Department of Oncology, The First Affiliated Hospital of Nanjing Medical University, Nanjing, Jiangsu, China; [4]Department of Oncology, The Affiliated Suzhou Hospital of Nanjing Medical University, Suzhou Municipal Hospital, Suzhou, China; [5]Gusu School, Nanjing Medical University, Suzhou, China; [6]Hepatobiliary Center, The First Affiliated Hospital of Nanjing Medical University, Nanjing, China; [7]Department of Oncology, Pukou Branch Hospital of Jiangsu Province Hospital, Nanjing, China

JHEP Reports **2023.** https://doi.org/10.1016/j.jhepr.2023.100763

Background & Aims: Immunotherapy is an option for the treatment of advanced biliary tract cancer (BTC), although it has a low response rate. In this post hoc analysis, we investigated the predictive value of an immuno-genomic-radiomics (IGR) analysis for patients with BTC treated with camrelizumab plus gemcitabine and oxaliplatin (GEMOX) therapy.
Methods: Thirty-two patients with BTC treated with camrelizumab plus GEMOX were prospectively enrolled. The relationship between high-throughput computed tomography (CT) radiomics features with immuno-genomic expression was tested and scaled with a full correlation matrix analysis. Odds ratio (OR) of IGR expression for objective response to camrelizumab plus GEMOX was tested with logistic regression analysis. Association of IGR expression with progression-free survival (PFS) and overall survival (OS) was analysed with a Cox proportional hazard regression.
Results: CT radiomics correlated with $CD8^+$ T cells (r = –0.72–0.71, p = 0.004–0.047), tumour mutation burden (TMB) (r = 0.59, p = 0.039), and *ARID1A* mutation (r = –0.58–0.57, p = 0.020–0.034). There was no significant correlation between radiomics and programmed cell death protein ligand 1 expression (p >0.96). Among all IGR biomarkers, only four radiomics features were independent predictors of objective response (OR = 0.09–3.81; p = 0.011–0.044). Combining independent radiomics features into an objective response prediction model achieved an area under the curve of 0.869. In a Cox analysis, radiomics signature [hazard ratio (HR) = 6.90, p <0.001], *ARID1A* (HR = 3.31, p = 0.013), and blood TMB (HR = 1.13, p = 0.023) were independent predictors of PFS. Radiomics signature (HR = 6.58, p <0.001) and $CD8^+$ T cells (HR = 0.22, p = 0.004) were independent predictors of OS. Prognostic models integrating these features achieved concordance indexes of 0.677 and 0.681 for PFS and OS, respectively.
Conclusions: Radiomics could act as a non-invasive immuno-genomic surrogate of BTC, which could further aid in response prediction for patients with BTC treated with immunotherapy. However, multicenter and larger sample studies are required to validate these results.
Impact and implications: Immunotherapy is an alternative for the treatment of advanced BTC, whereas tumour response is heterogeneous. In a *post hoc* analysis of the single-arm phase II clinical trial (NCT03486678), we found that CT radiomics features were associated with the tumour microenvironment and that IGR expression was a promising marker for tumour response and long-term survival.
Clinical trial number: *Post hoc* analysis of NCT03486678.

Keywords: Biliary duct cancer; Radiomics; Immunotherapy; Prognosis.
Received 18 January 2023; received in revised form 15 March 2023; accepted 30 March 2023; available online 22 April 2023
† These authors contributed equally.
* Corresponding author. Addresses: Hepatobiliary Center, The First Affiliated Hospital of Nanjing Medical University, Nanjing 210029, China, Tel.: +86-139-1392-8386 (X.-F. Wu); Department of Radiology, The First Affiliated Hospital of Nanjing Medical University, No. 300, Guangzhou Road, Nanjing, Jiangsu 210029, China, Tel.: +86-158-0515-1704 (Y.-D. Zhang); Department of Oncology, The First Affiliated Hospital of Nanjing Medical University, No. 300, Guangzhou Road, Nanjing, Jiangsu 210029, China; Department of Oncology, Pukou Branch Hospital of Jiangsu Province Hospital, Nanjing 211800, China; Gusu School, Nanjing medical University, Suzhou, 215006, China, Tel.: +86 135-8517-2066 (X.-F. Chen).
E-mail addresses: njmu_lqp@163.com (Q.-P. Liu), lytangj@126.com (J. Tang), yizhangchen@njmu.edu.cn (Y.-Z. Chen), guof123@126.com (F. Guo), maling@njmu.edu.cn (L. Ma), zjpanlanlan@163.com (L.-L. Pan), 835385247@qq.com (Y.-T. Tian), wuxf@njmu.edu.cn (X.-F. Wu), zhangyd3895@njmu.edu.cn (Y.-D. Zhang), chenxiaofengnjmu@163.com (X.-F. Chen).

Introduction

Biliary tract cancer (BTC) is a rare type of liver cancer accounting for ~3% of all gastrointestinal malignancies.[1] The global incidence rate of BTC is increasing, especially in Asian countries.[2] Given the aggressive tumour biology of BTC, more than 60% patients present beyond eligibility for curative-intent therapy.[2] For advanced BTC, systemic treatment such as gemcitabine plus cisplatin (GemCis) or gemcitabine plus oxaliplatin (GEMOX) represent the standard therapy.[3] However, chemotherapy-related toxicities affect patients' activities of daily living and result in high medical care costs. Additionally, the prognosis is far from satisfactory and the median overall survival (mOS) is only ~12 months.[2]

There is a rationale supporting the use of immunotherapy, such as immune checkpoint inhibitors (ICIs) against programmed cell death protein 1 (PD-1) in advanced BTC. Several clinical trials involving ICIs show promising results; for example, the phase III TOPAZ-1 trial combining GemCis plus durvalumab showed a significant improvement in mOS compared with GemCis plus placebo.[4] Based on the TOPAZ-1 trial, the National Comprehensive Cancer Network listed GemCis plus durvalumab as a category 1 recommendation for first-line therapy of advanced BTC.[2,5] Although BTC can be immunogenic, the infiltration of immunosuppressive immune cells is implicated in tumour immune escape. Moreover, the tolerogenic liver environment further enhances immunosuppression, because cancers may utilise this mechanism to promote immune tolerance and potentially resist ICI treatment.[6] In previous clinical trials, the activity of immunotherapy was limited, with the objective response rate ranging from 3% to 13%.[7]

Patient selection based on pretreatment biomarkers could help to maximise the efficacy, and reduce the number of patients who might not benefit from or even be harmed by ICIs. Several studies have shown that pre-existing tumoral and peritumoral immune infiltration correlates with patient response to ICIs.[6,8] Tumours with a distinct immune-inflamed phenotype are characterised by dense, functional $CD8^+$ T cell infiltration, enhanced interferon γ activity, and increased expression of immune checkpoint markers, such as programmed cell death ligand 1 (PD-L1). Thus, these tumours tend to respond to ICIs.[6,9] Furthermore, multimodal molecular profiling, including clinically relevant genomic profiling and immune transcriptomic data, could also be promising immune-related biomarkers.[3] However, obtaining adequate tumour tissue for molecular profiling is invasive and sometimes difficult. Thus, there is unmet need to develop better non-invasive and accurate biomarkers.

Radiomics are mathematically defined descriptors of tumour heterogeneity, and potential tools allowing non-invasive evaluation of tumour characteristics.[10,11] Encouraging results have been published on the potential utility of radiomics for non-invasively predicting pathological type and long-term survival in patients with BTC receiving resection treatment.[12,13] However, the correlation of radiomics features with immuno-genomic expression and clinical outcomes is rarely investigated in BTCs with immunotherapy. Thus, we evaluated the value of high-throughput computed tomography (CT) radiomics analyses for predicting the tumour microenvironment and outcomes in patients with advanced BTC treated with camrelizumab plus GEMOX.

Patients and methods

Patients

All patients with advanced BTC receiving the ICI camrelizumab plus GEMOX as first-line treatment were included from a single-arm open-label phase II clinical trial (NCT03486678), except for four patients, who lacked a pretreatment CT examination. Ethics committee approval was granted by Jiangsu Province Hospital ethics review board (protocol SHR1210-GEMOX-BTC-IIT03), and all patients provided written informed consent before study entry. All procedures involving human participants were performed in accordance with the 1975 Helsinki declaration and its later amendments. Detailed descriptions of the study design, eligibility criteria, and treatment schedules have been published previously.[14]

Candidate biomarkers, such as abundance of $CD8^+$ T cells, PD-L1 expression, tumour mutational burden (TMB), blood tumour mutational burden (bTMB), and some key commonly mutated genes in BTC, including *TP53*, *ARID1A*, *KRAS*, *RB1*, *CDKN2A*, *PIK3CA*, *SMAD4*, *MCL1*, *TERT*, *EPHA2*, *ERBB2*, *KMT2B*, *NTRK1* and *SMARCA4*, were obtained from baseline biopsy specimens and blood samples to assess the immunotherapy of BTC. Details of the measurement of those biomarkers are provided elsewhere.[14,15]

CT acquisition

All participants underwent the same baseline abdominal contrast-enhanced CT examination on a multi-slice spiral CT (MSCT) scanner (SIEMENS SOMATOM Definition AS 128 CT, Forchheim, Germany) within 1 week before starting treatment with camrelizumab plus GEMOX. The scanning conditions were as follows: tube voltage,120 kVp; effective tube current–exposure time product, 180 mAs^{eff}; rotation time, 0.5 s; field of view, 350 × 350 mm; matrix, 512 × 512; and reconstruction section thickness, 1.5 mm. MSCT was performed with a non-ionic iodine contrast agent (Iopromide 300 mg I/ml) injected via an antecubital vein at a rate of 3.0 ml/s using a CT-compatible power injector for a total volume of 90–120 ml (1.5 ml/kg of body weight). The scanning delay for arterial phase was determined using the built-in automatic bolus-triggering software of the scanner. Arterial phase scanning automatically began 10 s after the trigger attenuation threshold (100 Hounsfield units; HU) was reached at the level of the supraceliac abdominal aorta. Portal-venous phase scanning began 40–60 s after arterial phase scanning.

Radiomics analysis

Tumour segmentation was performed by a board-certified subspecialist (YDZ, with 15 years of experience in liver imaging) and 1.5-mm portal-venous phase CT images were analysed using in-house software (ONCO IMAG ANLY v 2.0; Shanghai Key Laboratory of MRI, ECNU, Shanghai, China) written with Python 3.6.1 (www.python.org). The software allows the semi-automatic identification of the volume of interest (VOI) of the tumour with a combination of an automatic segmentation algorithm and a manual approach. To capture quantitative data from the tumour microenvironment, we dilated the tumour region masks slightly with a 5-mm external extension of the mask contours. Large vessels, adjacent organs, and air cavities were excluded if not infiltrated by the tumour. A central challenge in tumour segmentation is the presence of ambiguous regions, where the true tumour boundary cannot be deduced from the image and, thus, multiple equally plausible interpretations exist. To fill this gap, the VOI of each lesion was drawn twice with 2-week intervals by the same radiologist. Regional identification overlapping was identified in two instances as the authorised VOI of the targeted lesion.

Volumetric radiomics features were analysed from target VOIs using an open-source Python package (Pyradiomics 2.1.2). Image normalisation was performed using a method that remapped the histogram to fit within μ ± 3σ (μ: mean grey-level within the VOI and σ: grey-level standard deviation). A total of 944 radiomics features, such as intensity, shape, texture, and wavelets, were computed for target volume based on the texture analysis methods available in the software package (Text S1).

Clinical outcomes

The primary endpoint was the objective response of BTC to the camrelizumab plus GEMOX treatment, which was evaluated according to RECIST version 1.1, and the best overall response was used for subsequent logistic regression analysis.[16] Progression-free survival (PFS) and overall survival (OS) were defined as the time from first drug administration to the first documented disease progression or to death from any cause, respectively. The definition criteria are detailed in full in the trial protocol (NCT03486678).[14]

Statistical analysis

Given that the endpoints of the clinical trial were safety, objective response, and survival, the sample size was determined based on clinical considerations. In this *post hoc* analysis, Spearman correlation matrix analysis was performed to determine the relationship between radiomics features and abundance of $CD8^+$ T cells, PD-L1 expression, TMB of tumour tissue and blood, and expression of 14 key genes (*TP53*, *ARID1A*, *KRAS*, *RB1*, *CDKN2A*, *PIK3CA*, *SMAD4*, *MCL1*, *TERT*, *EPHA2*, *ERBB2*, *KMT2B*, *NTRK1*, and *SMARCA4*), as detailed elsewhere.[14] Stepwise logistic regression (LR) analysis and area under the receiver operating characteristic (AUROC) curves were used to determine the performance of IGR biomarkers for tumour response. In addition, we used sensitivity and specificity as the evaluation metrics. Predictors for PFS and OS were determined by Cox regression analysis; then, a least absolute shrinkage and selection operator (Lasso) Cox algorithm was further used to compile PFS and OS radiomics survival signatures from significant variables in Cox regression,[17] using Eq. 1:

$$Radiomics\ signature = \sum_0^i \beta i Xi \quad [1]$$

where βi is the Lasso Cox coefficient and Xi is the value of the selected radiomics feature.

Significant predictors were further integrated into prediction and prognostic models for objective response and survival via multivariate regression analysis. Model performance was evaluated with AUROC and concordance index based on fivefold cross-validation. Kaplan–Meier curves and log-rank tests were used to plot and compare the survival curves, respectively. Two-sided p values <0.05 were considered statistically significant, and p values were adjusted for multiple correlations via false discovery rate (FDR) adjustment. Statistical analysis was performed using R software (version 4.0.4; R Foundation for Statistical Computing, Vienna, Austria) and SPSS (version 25, IBM Analytics, Armonk, NY, USA).

Results

Baseline patient characteristics

All 32 patients enrolled completed the full course of camrelizumab plus GEMOX treatment and CT examination. The baseline characteristics of the participants are summarised in Table 1. As of August 1, 2020, an objective response to camrelizumab plus GEMOX had been observed in 16 (50.0%) patients. Thirty (93.7%) patients developed documented disease progression and 25 (78.1%) patients passed away. The median PFS and OS of the cohort were 6.0 (95% CI 4.3–7.1) and 12.1 (95% CI 8.0–17.8) months, respectively.

Correlation of radiomics with immuno-genomic expression

Radiomics including one texture (r = –0.72, p = 0.004), 11 gradient (r = –0.67–0.71, p = 0.005–0.047), and 13 wavelet (r = –0.72–0.70, p = 0.004-0.046) features were significantly associated with the quantitative expression of $CD8^+$ T cells (Fig. 1A). One texture feature had significant association with the TMB of tumour tissue (r = 0.59, p = 0.039) (Fig. 1A). No significant correlation was observed between radiomics features and expression of PD-L1 (p >0.96). Among the 32 participants, *TP53* was the gene with the highest mutation frequency (14/32, 43.8%), followed by *ARID1A*, *KRAS*, and *RB1* (Fig. S1). Correlation analysis demonstrated that radiomics features were only significantly correlated with *ARID1A* mutation (r = –0.58–0.57; p = 0.020–0.034) (Fig. 1A). No significant correlation was observed between radiomics and genomic expression, such as that of *TP53*, *KRAS*, *RB1*, *CDKN2A*, *PIK3CA*, *SMAD4*, *MCL1*, *TERT*, *EPHA2*, *ERBB2*, *KMT2B*, *NTRK1*, and *SMARCA4* (p >0.31). Details of the IGR correlation analysis are summarised in Table 2.

Predictors of tumour response

In the LR analysis, four wavelet-related radiomics features (OR = 0.09–3.81, p = 0.011–0.044) showed a significant association with the objective response of BTC to camrelizumab plus GEMOX. There was no significant association of immune-genomic expression with objective response to treatment (p >0.21) (Fig. 1B). Using the optimal cut-off value that maximises the Youden index, the predictive performance of four significant radiomic predictors for objective response assessment is summarised in Table 3. Combining these features into a response prediction model achieved a mean AUROC of 0.869 in cross-validation (Fig. S2).

Predictors of PFS and OS

In the Lasso Cox analysis, five radiomics features (one gradient, one texture, and three wavelet features) were selected as the leading predictors of PFS. Those five radiomics features were compiled into a survival radiomics signature (RadPFS) as follow:

Table 1. Baseline characteristics of trial participants.

Characteristics	No. of patients (n = 32)
Sex	
Male	22 (68.8%)
Female	10 (31.2%)
Age	
≤60 years	8 (25%)
>60 years	24 (75%)
Primary site	
Cholangiocarcinoma	20 (62.5%)
Gallbladder cancer	12 (37.5%)
Tumour response	
Partial response	16 (50.0%)
Stable disease	13 (40.6%)
Progressive disease	3 (9.4%)

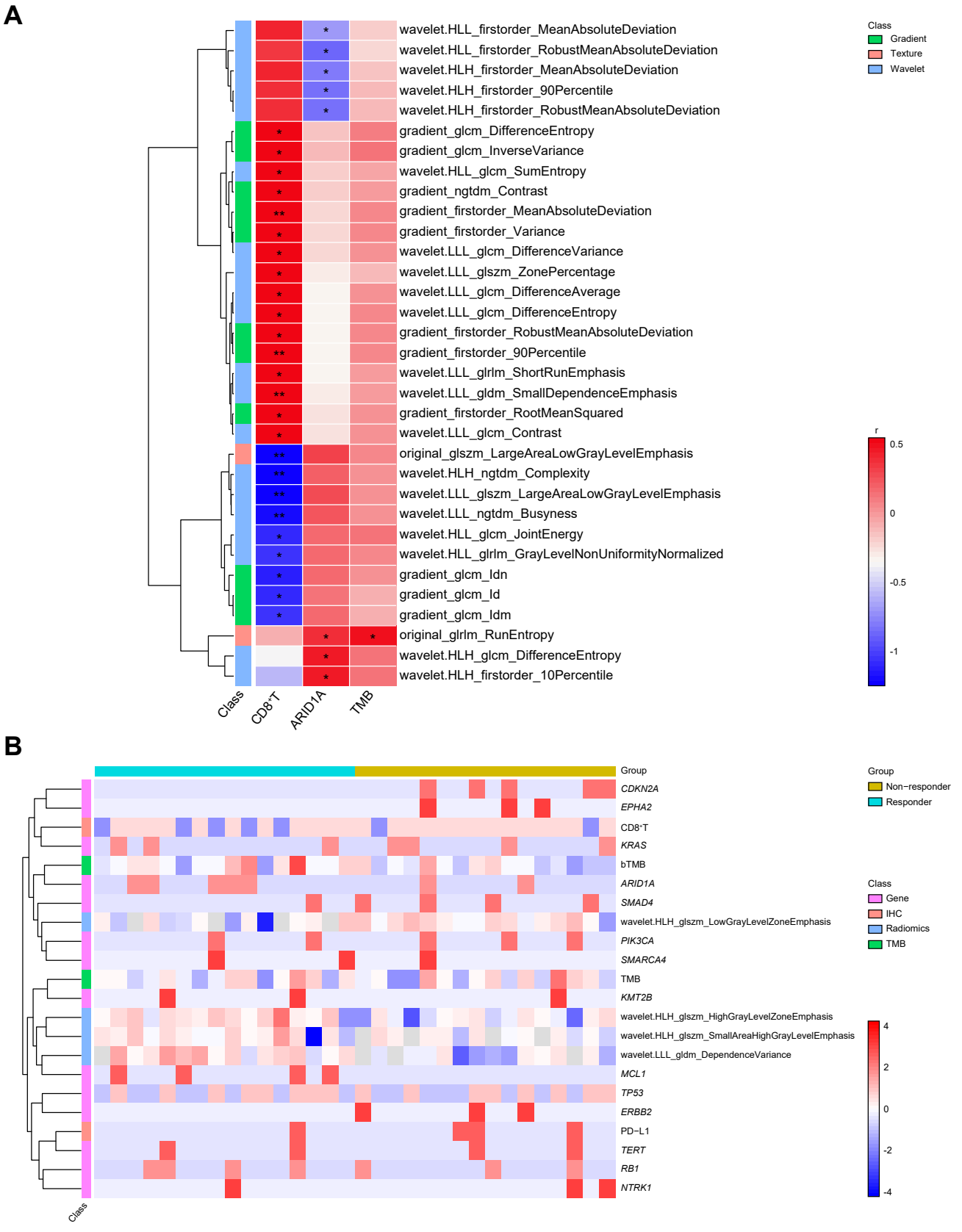

Fig. 1. Significant radiomics features with immuno-genomic and tumor response. (A) Correlation of significant radiomics features with $CD8^+$ T cell, TMB and *ARID1A* expression. (B) Heatmap of significant radiomics features and Immuno-Genomic markers in responder *vs.* non-responder group. $^*p$ <0.05; $^{**}p$ <0.001; *p* values from spearman correlation analysis. TMB, tumor mutation burden.

Table 2. Significant correlations of radiomics features with immune and gene expression in 32 patients with biliary tract cancer.

Biomarker	Radiomics feature	*r*	*p* value*
$CD8^+$ T cell	*Texture*		
	original_glszm_LargeAreaLowGrayLevelEmphasis	-0.716	0.004
	Gradient		
	gradient_glcm_Idn	-0.674	0.022
	gradient_glcm_Id	-0.663	0.033
	gradient_glcm_Idm	-0.658	0.039
	gradient_firstorder_Variance	0.653	0.047
	gradient_glcm_DifferenceEntropy	0.659	0.038
	gradient_glcm_InverseVariance	0.663	0.033
	gradient_firstorder_RootMeanSquared	0.667	0.029
	gradient_ngtdm_Contrast	0.682	0.016
	gradient_firstorder_RobustMeanAbsoluteDeviation	0.685	0.015
	gradient_firstorder_MeanAbsoluteDeviation	0.697	0.009
	gradient_firstorder_90Percentile	0.708	0.005
	Wavelet		
	wavelet.HLH_ngtdm_Complexity	-0.716	0.004
	wavelet.LLL_glszm_LargeAreaLowGrayLevelEmphasis	-0.710	0.005
	wavelet.LLL_ngtdm_Busyness	-0.698	0.008
	wavelet.HLL_glcm_JointEnergy	-0.666	0.030
	wavelet.HLL_glrlm_GrayLevelNonUniformityNormalized	-0.658	0.039
	wavelet.LLL_glszm_ZonePercentage	0.653	0.046
	wavelet.LLL_glcm_DifferenceAverage	0.654	0.045
	wavelet.HLL_glcm_SumEntropy	0.662	0.034
	wavelet.LLL_glrlm_ShortRunEmphasis	0.670	0.025
	wavelet.LLL_glcm_Contrast	0.671	0.025
	wavelet.LLL_glcm_DifferenceVariance	0.671	0.025
	wavelet.LLL_glcm_DifferenceEntropy	0.674	0.022
	wavelet.LLL_gldm_SmallDependenceEmphasis	0.698	0.008
ARID1A	*Wavelet*		
	wavelet.HLL_firstorder_RobustMeanAbsoluteDeviation	-0.585	0.020
	wavelet.HLH_firstorder_90Percentile	-0.577	0.020
	wavelet.HLH_firstorder_RobustMeanAbsoluteDeviation	-0.577	0.020
	wavelet.HLH_firstorder_MeanAbsoluteDeviation	-0.553	0.021
	wavelet.HLH_glcm_DifferenceEntropy	0.536	0.021
	wavelet.HLH_firstorder_10Percentile	0.569	0.021
	wavelet.HLL_firstorder_MeanAbsoluteDeviation	-0.512	0.034
Tumour mutation burden	*Texture*		
	original_glrlm_RunEntroy	0.590	0.039

TMB, tumour mutation burden.
* *p* values from Spearman correlation analysis with false discovery rate adjustment.

RadPFS = −0.006 × gradient_glcm_MCC - 0.019 × original_gldm_DependenceVariance + 0.099 × wavelet.HHL_glcm_DifferenceAverage + 0.262 × wavelet.HHL_glcm_Imc2 + 0.562 × wavelet.HHL_glcm_MCC.

Detailed information of feature selection and corresponding coefficients is provided in Table S1 and Fig. S1.

In the multivariate Cox regression analysis, RadPFS (hazard ratio [HR] = 6.90, 95% CI 3.08–15.47; p <0.001), *ARID1A* mutation (HR = 3.31, 95% CI 1.30–8.44; p = 0.013), and bTMB (HR = 1.13, 95% CI 1.02–1.24; p = 0.023) were identified as independent predictors of PFS (Fig. 2A). Using the median as the cut-off value of continuous variables, Kaplan–Meier curves of the referring predictors were established (Fig. 2B–D). A prognostic model combining these features achieved a mean concordance index of 0.677 (Fig. S2).

Similarly, 10 radiomics features (one intensity, two texture, one gradient, and six wavelet features) were retained using Lasso Cox analysis and the corresponding survival signature (*i.e.* RadOS) was established as follows (see also Table S2 and Fig. S1):

RadOS = 0.023 × gradient_ngtdm_Busyness + 0.151 × firstorder_InterquartileRange + 0.340 × original_glcm_ClusterTendency − 0.049 × riginal_glszm_SizeZoneNonUniformityNormalized − 0.599 × wavelet.HHL_glcm_Imc1 + 0.123 × wavelet.HHL_glcm_MCC + 0.105 × wavelet.HLH_glszm_ZoneEntropy − 0.086 × wavelet.LLH_gldm_DependenceEntropy − 0.087 × wavelet.LLH_glrlm_RunPercentage + 0.021 × wavelet.LLL_glcm_Correlation.

In the multivariate Cox regression analysis, RadOS (HR = 6.58; 95% CI 3.22–13.44; p <0.001) and $CD8^+$ T cells (HR = 0.22; 95% CI 0.08–0.61; p = 0.004) were independent predictors of OS (Fig. 2E;

Table 3. Immuno-genomic-radiomics predicters significantly associated with tumour response.

Radiomics feature	OR (95% CI)	*p* value*	AUROC	SEN (%)	SPE (%)
wavelet.HLH_glszm_HighGrayLevelZoneEmphasis	0.09 (0.01–0.73)	0.024	0.760	93.8	56.3
wavelet.HLH_glszm_LowGrayLevelZoneEmphasis	3.81 (1.23–11.8)	0.020	0.760	93.8	56.3
wavelet.HLH_glszm_SmallAreaHighGrayLevelEmphasis	0.28 (0.08–0.97)	0.044	0.730	81.3	62.5
wavelet.LLL_gldm_DependenceVariance	0.15 (0.04–0.65)	0.011	0.840	100.0	62.5

AUROC, area under the receiver operating curve; OR, odds ratio; SEN, sensitivity; SPE, specificity.
* *p* values from logistic regression.

Kaplan–Meier curves are depicted in Fig. 2F and G). A prognostic model integrating these features produced a mean concordance index of 0.681 (Fig. S2).

RadPFS and RadOS remained significant predictors for survival in a subgroup of patients with gallbladder cancer and cholangiocarcinoma. In the gallbladder cancer group, RadPFS could further stratify patients with significant distinct survival patterns with a median PFS of 6.93 (95% CI 5.98–10.12) *vs.* 3.58 (95% CI, 3.22–4.17) in the low-risk *vs.* high-risk group, respectively (log-rank $p = 0.035$) (Fig. 3A); and RadOS stratified patients with a median OS of 21.95 (95% CI 7.98–21.95) *vs.* 7.66 (95% CI 6.74–13.04) in the low-risk *vs.* high-risk group, respectively (log-rank $p = 0.035$) (Fig. 3B). Similarly, in the cholangiocarcinoma group, RadPFS stratified patients with a median PFS of 9.99 (95% CI 6.18–13.90) *vs.* 4.27 (95% CI 4.01–5.42) in the low-risk *vs.* high-risk group, respectively (log-rank $p = 0.002$) (Fig. 3C); and RadOS stratified patients with a median OS of 17.84 (95% CI 12.09–21.03) *vs.* 7.23 (95% CI 6.18–12.65) in the low-risk *vs.* high-risk group, respectively (log-rank $p = 0.004$) (Fig. 3D).

Discussion

In this prospective study, we evaluated the potential value of IGR, especially CT-based radiomics features, for non-invasively predicting post-treatment outcomes of patients with advanced BTC treated with camrelizumab plus GEMOX. We found that several radiomics features were correlated with immuno-genomic expression of BTC. Moreover, radiomics features were also identified as independent predictors of treatment response and survival. These results demonstrated that high-throughput radiomics analysis of CT could be a non-invasive surrogate for immuno-genomics biomarkers and aid in making individualised treatment decisions for immunotherapy in patients with BTC.

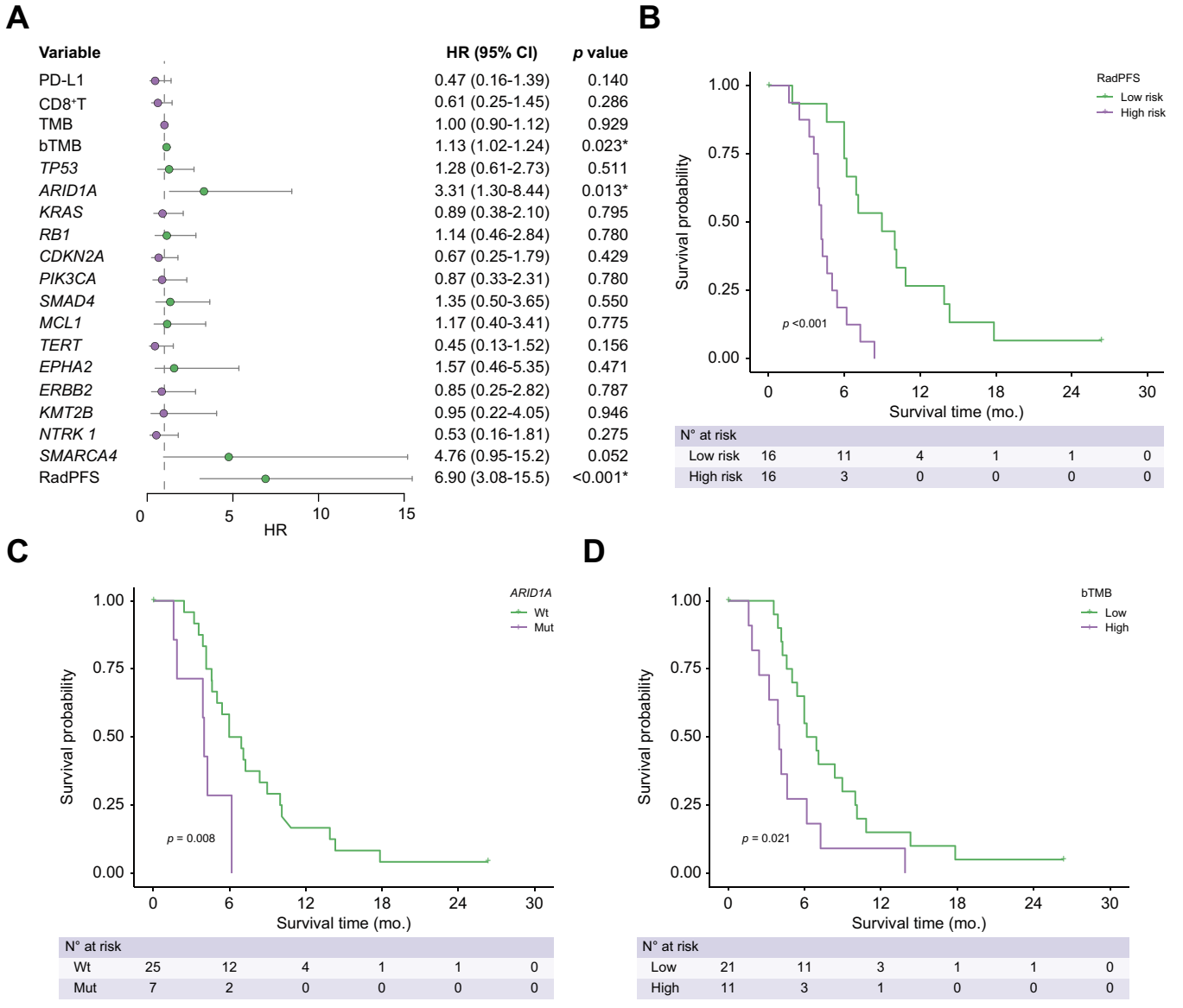

Fig. 2. Forest plots and Kaplan-Meier curves of predictors for PFS and OS. (A) Forest plot of predictors for PFS. (B-D) Kaplan-Meier curves of significant variables for PFS. (E) Forest plot of predictors for OS. (F, and G) Kaplan-Meier curves of significant variables for OS. *p* values from Cox regression or Log-rank test.

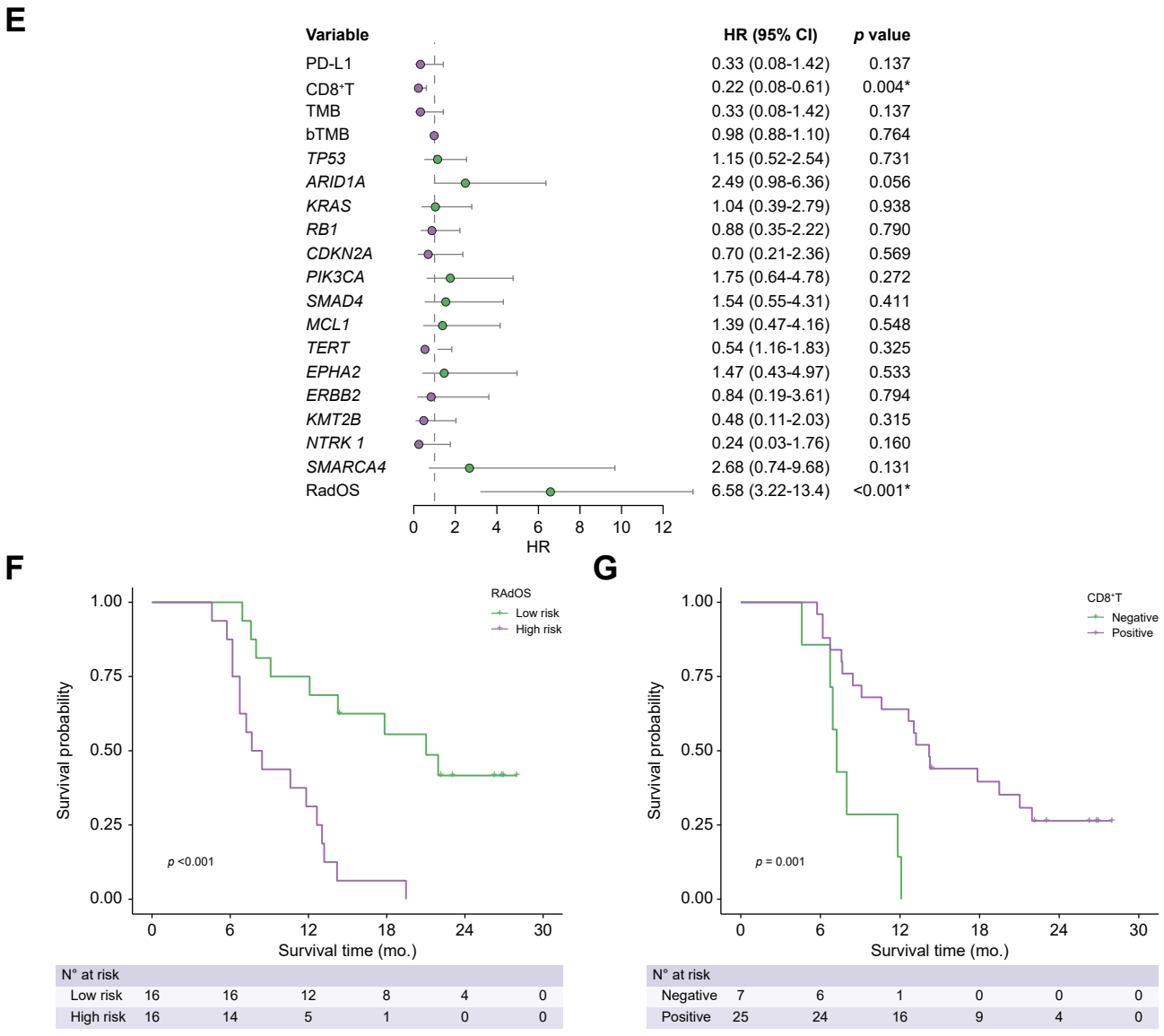

Fig. 2 (*continued*).

Chemotherapy plus ICIs is a promising treatment approach and has become the standard first-line choice for advanced BTC based on the results from the phase III TOPAZ-1 trial.[5,7] Give that the tumour immune microenvironment has a vital role in tumour development, progression, and treatment efficacy, there is increasing interest in characterising the microenvironment of BTC.[2] In our study, texture features reflecting tumour neovascularisation and heterogeneity were correlated with the abundance of $CD8^+$ T cells, which was in accordance with a previous study using pre-treatment radiomics to predict the level of $CD8^+$ T cells in hepatocellular carcinoma.[18] In contrast to previous studies, none of the radiomics features were significantly correlated with PD-L1 status.[18,19] These conflicting results could be explained, in part, by the fact that we used multiple testing to select features, whereas previous studies compiled radiomics score combining several radiomics features. *ARID1A* mutation has been identified as important genomic event in BTC and, interestingly, radiomics was correlated with *ARID1A* mutation, but not with other genomic alterations. This can be explained, in part, by the fact that the subtypes of BTCs have different genomic characteristics, and more correlations could be mined in radiomics subgroup analyses.[2]

Clinical outcomes of ICI treatment are heterogenous. Thus, we assessed the predictive ability of radiomics features for treatment response and survival. Previous studies mainly focused on the predictive and prognostic role of biomarkers, such as genomic alterations and the molecular and immune profiling of the tumour microenvironment.[2,20] The association of radiomics features with objective response of BTC to camrelizumab plus GEMOX has been less investigated. In this study, wavelet-related radiomics features reflecting tumour heterogeneity and enhancement were the only independent predictors of tumour response among a series of IGR factors. This implied that high-throughput radiomics analysis of CT could be an alternative pathway to conventional genomic biomarkers to select patients who are candidates for ICI therapies. In addition, radiomics

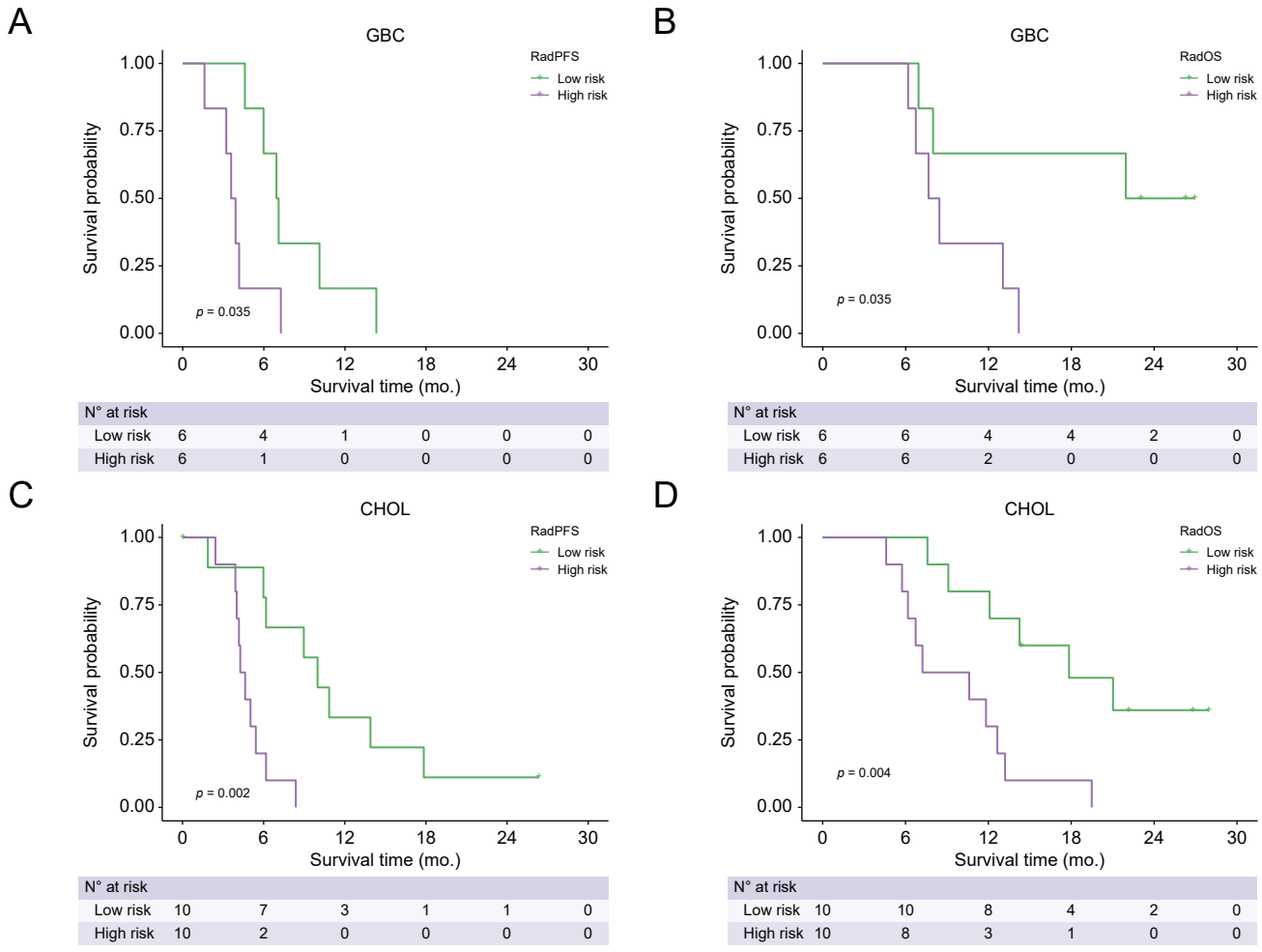

Fig. 3. Prognostic performance of radiomics survival signatures in gallbladder cancer and cholangiocarcinoma subgroup. (A-B) Kaplan-Meier curves of radiomics signature in gallbladder cancer group. (C-D) Kaplan-Meier curves of radiomics signature in cholangiocarcinoma cancer group. *p* values from Log-rank test. CHOL, cholangiocarcinoma; GBC, gallbladder cancer.

features were determined to be associated with state-of-the-art prognostic biomarkers, such as immune cell expression and gene mutations. Accordingly, hybrid radiomics scores were independent predictors of PFS and OS, which was in accordance with previous studies.[21,22] In clinical practice, imaging examination is already routinely performed of patients with BTC. Thus, CT radiomics analysis could be a cost-effective and non-invasive alternative for prognosis prediction.

There are several limitations to our study. First, the sample size was relatively small in this prospective exploratory study, which could influence the reliability of our developed models.[23,24] Thus, larger sample sizes and independent test sets are required to validate our results. Second, the segmentation of lesions was semi-automatic, which has inter-reader variability and time-consuming problems, and the predictive ability of radiomics is restricted by the heterogeneity of scan protocols. Advances in computer imaging segmentation algorithms and standardisation of radiomics analysis workflow could make our approach a reality. Third, multiparametric magnetic resonance imaging can provide more qualitive and quantitate features, which might have better predictive and prognostic performance in the tumour microenvironment and for clinical outcomes.

In conclusion, our study found that pretreatment CT radiomics features might correlate with BTC immune-genomic characteristics, and allow the prediction of immunotherapy outcomes. Radiomics analysis could be an alternative to conventional approaches for making individualised decisions in patients with advanced BTC in terms of treatment with ICI. However, multicenter and larger sample-sized studies are required to validate these results.

Abbreviations

BTC, biliary tract cancer; CT, computed tomography; FDR, false discovery rata; GEMOX, gemcitabine and oxaliplatin; HR, hazard ratio; ICI, immune checkpoint inhibitor; IGR, immuno-genomic-radiomics; Lasso, least absolute shrinkage and selection operator; LR, logistic regression; OR, odds ratio; OS, overall survival; PD-1, programmed cell death protein 1; PD-L1,

programmed cell death ligand 1; PFS, progression-free survival; TMB, tumour mutation burden; VOI, volume of interest.

Financial support
The study was funded by Jiangsu province 333 high level Talents Project (XC; YZ), Innovation Funds From Chinese Society Of Clinical Oncology Youth Committee (Y-Young2019-060 to XC), Beijing Xisike Clinical Oncology Research Foundation (Y-HR2019-0367 to XC), and the National Natural Science Foundation of China (82102981 to LM; 82272082 to YZ).

Conflicts of interest
The authors declare no potential conflicts of interest in this study.

Please refer to the accompanying ICMJE disclosure forms for further details.

Authors' contributions
Study conception: Q-PL, JT, W-XF, Y-DZ, X-FC. Data collection: Q-PL, JT, Y-ZC, FG, LM, L-LP, Y-TT, X-FW, Y-DZ, X-FC. Data analysis: Q-PL, JT, Y-ZC, FG, LM, L-LP, Y-TT, X-FW, Y-DZ, X-FC. Administrative support: X-FW, Y-DZ, X-FC. Manuscript drafting: Q-PL, Y-DZ, X-FC. All authors read and approved the final version of the manuscript.

Data availability statement
The imaging studies and clinical data used for algorithm development are not publicly available, because they contain private patient health information. Interested users may request access to these data, where institutional approvals along with signed data use agreements and/or material transfer agreements may be needed/negotiated. Derived result data supporting the findings of this study are available upon reasonable request from the corresponding authors.

Supplementary data
Supplementary data to this article can be found online at https://doi.org/10.1016/j.jhepr.2023.100763.

References
Author names in bold designate shared co-first authorship

[1] Adeva J, Sangro B, Salati M, Edeline J, La Casta A, Bittoni A, et al. Medical treatment for cholangiocarcinoma. Liver Int 2019;39(Suppl 1):123–142.
[2] Scott AJ, Sharman R, Shroff RT. Precision medicine in biliary tract cancer. J Clin Oncol 2022;40:2716–2734.
[3] Valle JW, Kelley RK, Nervi B, Oh DY, Zhu AX. Biliary tract cancer. Lancet 2021;397:428–444.
[4] Oh D-Y, He AR, Qin S, Chen L-T, Okusaka T, Vogel A, et al. A phase 3 randomized, double-blind, placebo-controlled study of durvalumab in combination with gemcitabine plus cisplatin (GemCis) in patients (pts) with advanced biliary tract cancer (BTC): TOPAZ-1. J Clin Oncol 2022;40:378.
[5] Roth GS, Neuzillet C, Sarabi M, Edeline J, Malka D, Lièvre A. Cholangiocarcinoma: what are the options in all comers and how has the advent of molecular profiling opened the way to personalised medicine? Eur J Cancer 2023;179:1–14.
[6] Loeuillard E, Conboy CB, Gores GJ, Rizvi S. Immunobiology of cholangiocarcinoma. JHEP Rep 2019;1:297–311.
[7] Bang Y-J, Ueno M, Malka D, Chung HC, Nagrial A, Kelley RK, et al. Pembrolizumab (pembro) for advanced biliary adenocarcinoma: results from the KEYNOTE-028 (KN028) and KEYNOTE-158 (KN158) basket studies. J Clin Oncol 2019;37:4079.
[8] **Carapeto F**, **Bozorgui B**, Shroff RT, Chagani S, Solis Soto L, Foo WC, et al. The immunogenomic landscape of resected intrahepatic cholangiocarcinoma. Hepatology 2022;75:297–308.
[9] Sanmamed MF, Chen L. A paradigm shift in cancer immunotherapy: from enhancement to normalization. Cell 2018;175:313–326.
[10] **Chen S**, **Feng S**, Wei J, Liu F, Li B, Li X, et al. Pretreatment prediction of immunoscore in hepatocellular cancer: a radiomics-based clinical model based on Gd-EOB-DTPA-enhanced MRI imaging. Eur Radiol 2019;29:4177–4187.
[11] Gillies RJ, Kinahan PE, Hricak H. Radiomics: images are more than pictures, they are data. Radiology 2016;278:563–577.
[12] King MJ, Hectors S, Lee KM, Omidele O, Babb JS, Schwartz M, et al. Outcomes assessment in intrahepatic cholangiocarcinoma using qualitative and quantitative imaging features. Cancer Imaging 2020;20:43.
[13] Yang C, Huang M, Li S, Chen J, Yang Y, Qin N, et al. Radiomics model of magnetic resonance imaging for predicting pathological grading and lymph node metastases of extrahepatic cholangiocarcinoma. Cancer Lett 2020;470:1–7.
[14] **Chen X**, **Wu X**, Wu H, Gu Y, Shao Y, Shao Q, et al. Camrelizumab plus gemcitabine and oxaliplatin (GEMOX) in patients with advanced biliary tract cancer: a single-arm, open-label, phase II trial. J Immunother Cancer 2020;8:e001240.
[15] **Chen X**, **Wang D**, **Liu J**, **Qiu J**, Zhou J, Ying J, et al. Genomic alterations in biliary tract cancer predict prognosis and immunotherapy outcomes. J Immunother Cancer 2021;9:e003214.
[16] Schwartz LH, Litière S, de Vries E, Ford R, Gwyther S, Mandrekar S, et al. RECIST 1.1-Update and clarification: from the RECIST committee. Eur J Cancer 2016;62:132–137.
[17] Tibshirani R. The lasso method for variable selection in the Cox model. Stat Med 1997;16:385–395.
[18] **Liao H**, **Zhang Z**, Chen J, Liao M, Xu L, Wu Z, et al. Preoperative radiomic approach to evaluate tumor-infiltrating CD8(+) T cells in hepatocellular carcinoma patients using contrast-enhanced computed tomography. Ann Surg Oncol 2019;26:4537–4547.
[19] Zhang J, Wu Z, Zhang X, Liu S, Zhao J, Yuan F, et al. Machine learning: an approach to preoperatively predict PD-1/PD-L1 expression and outcome in intrahepatic cholangiocarcinoma using MRI biomarkers. ESMO Open 2020;5:e000910.
[20] Lin ZF, Qin LX, Chen JH. Biomarkers for response to immunotherapy in hepatobiliary malignancies. Hepatobiliary Pancreat Dis Int 2022;21:413–419.
[21] Ji GW, Zhang YD, Zhang H, Zhu FP, Wang K, Xia YX, et al. Biliary tract cancer at CT: a radiomics-based model to predict lymph node metastasis and survival outcomes. Radiology 2019;290:90–98.
[22] Li Q, Che F, Wei Y, Jiang HY, Zhang Y, Song B. Role of noninvasive imaging in the evaluation of intrahepatic cholangiocarcinoma: from diagnosis and prognosis to treatment response. Expert Rev Gastroenterol Hepatol 2021;15:1267–1279.
[23] Riley RD, Ensor J, Snell KIE, Harrell Jr FE, Martin GP, Reitsma JB, et al. Calculating the sample size required for developing a clinical prediction model. BMJ 2020;368:m441.
[24] Riley RD, Collins GS, Ensor J, Archer L, Booth S, Mozumder SI, et al. Minimum sample size calculations for external validation of a clinical prediction model with a time-to-event outcome. Stat Med 2022;41:1280–1295.